

MECHANICAL MODELLING AND LIFE CYCLE OPTIMISATION OF SCREEN PRINTING

ESZTER HORVATH, GABOR HARSANYI

Budapest University of Technology and Economics, Department of Electronics Technology, Budapest, Hungary
e-mail: horvathe@ett.bme.hu; harsanyi@ett.bme.hu

GABOR HENAP

Budapest University of Technology and Economics, Department of Applied Mechanics, Budapest, Hungary
e-mail: henap@mm.bme.hu

ADAM TOROK

Budapest University of Technology and Economics, Department of Transport Economics, Budapest, Hungary
e-mail: atorok@kgazd.bme.hu

The application of thick film pastes and adhesives is a screen printing method in the mass production of thick films and low temperature co-fired ceramic circuits. During this process, the paste is printed by a rubber squeegee onto the surface of the substrate through a stainless steel metal screen masked by photolithographic emulsion. We consider the off-contact screen printing method in this paper, because it is now the standard printing method in the microelectronics industry. In our research a Finite Element Model (FEM) was created in ANSYS Multiphysics software to investigate screen deformation and to reduce stress in the screen in order to extend its life cycle. An individual deformation measuring setup was designed to validate the FEM model of the screen. By modification of geometric parameters of the squeegee, the maximal and the average stress in the screen can be reduced. Furthermore, tension of the screen decreases in its life cycle, which results in worse printing quality. The compensation of this reducing tension and the modified shape of the squeegee are described in this paper. Using this approach, the life cycle of the screen could be extended by decreased mechanical stress and optimised off-contact.

Key words: screen printing, FEM, thick film, optimisation, life cycle

1. Introduction

The screen printing is the most widespread and common additive layer deposition and patterning method in thick film technology.

A thick film circuit usually contains conductive lines, resistive and dielectric layers. Screen printing technology provides the most cost effective facility of applying and patterning different layers for hybrid electronics industry. Due to its simple technology and relative cheapness, it is still widely used in the mass assembly of recent electronic circuits. The screen-printing is ideal as a manufacturing approach for microfluidic elements also used in the field of clinical, environmental or industrial analysis (Albareda-Sirvent *et al.*, 2000), in sensors (Viricelle, 2006) and in solar cells (Krebs, 2007).

The paste printing is carried out by a screen printer machine. The screen is strained onto an aluminium frame and the thick film paste is pressed onto the substrate through the screen not covered by emulsion by a printing squeegee. The squeegee has a constant speed and pushes the screen with contact force. The material of the screen can be a stainless steel or polymer. The design of the printed layer is realized with a negative emulsion mask on the screens. There are two main techniques of the screen printing:

- off-contact, where the screen is warped with a given tension above the substrate;
- contact, where the screen is in full contact with the substrate.

The contact screen-printing is less advantageous in general, because due to the lift off of the screen, damage of the high resolution pattern is often detected.

In the case of the off-contact screen-printing, some paste is applied on the top of the screen in the front of the polymer squeegee. While the squeegee is moving forward, it deforms the screen downwards until it comes into contact with the substrate beneath. The paste is pushed along in front of the squeegee and pushed through the screen not covered by the emulsion pattern onto the substrate. The screen and substrate separate behind the squeegee. The off-contact screen printing process is demonstrated in Fig. 1.

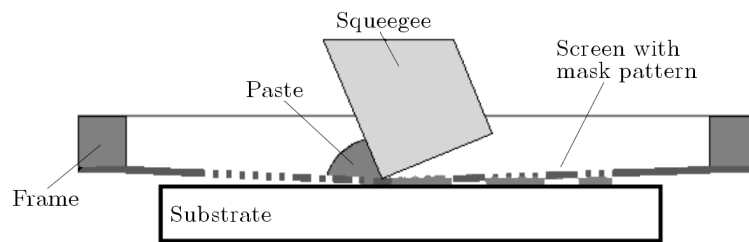


Fig. 1. The squeegee pushes the paste on the screen and presses it through the openings

Since the '60s several experiments and models of the printing process have been evaluated. The optimisation of screen printing was mainly achieved by experimental evaluation without the advantage of numerical models. That empirical optimisation method was described by Kobs and Voigt in 1970, they appointed more than 50 variables and combined the most important ones almost 300 different ways and compared the effects of them. Those investigations offer a enormous empirical database but general rules for screen-printing cannot be created from this without models. Miller (1969) investigated the amount of paste printed on the substrate in function of paste rheology, mesh size and line width. Others examined the influence of squeegee angle and characteristic on the thickness of the deposited paste (Benson, 1969) and the effect of the screen on fine scale printed patterns (Bacher, 1986).

The first efforts to achieve a theoretical description of the screen printing process were made by Riemer more than 20 years ago (1988, 1989). His mathematical models of the screen-printing process based fundamentally on a Newtonian viscous fluid scraping model (Taylor, 1962). This model was extended by others (Riedler, 1983; Jeong and Kim, 1985), although they did not take into account the flexibility of the screen, which is an essential feature of the process. None of these models deals with the effect of geometry in the screen printing process. The repetitive characteristic of the printing process requires taking into consideration the effect of the cyclic load. In this work, a mechanical model is presented with similar geometry to the off-contact screen printing process. In this model, the mechanical behaviour of the screen is in the focus instead of the paste deposition phase. Furthermore, our model effectively concerns the geometry of the knife.

2. Experimental

2.1. Material parameters of screen

The first step of the model constitution is to define the geometries and obtain the mechanical parameters of the screen. The geometric features and the initial strain - which warps it onto an aluminium frame - are realised by the manufacturing process.

In order to decrease screen tension deviation during the printing, the screen is tightened onto the aluminium frame with the thread orientation of 45° to the printing direction. Therefore, the load distribution is more homogeneous between the threads.

The elastic (Young) modulus of the screen is determined using the modified Voigt expression

$$E_c = \eta E_f V_f + E_m(1 - V_f) \quad (2.1)$$

where $E_m = 690$ MPa is the elastic modulus of the emulsion, $E_f = 193$ GPa is the elastic modulus of the stainless steel, V_f is the volume fraction of the stainless steel and η is the Krenchel efficiency factor (Cox, 1952; Krenchel, 1964). In the case of $\Theta_1 = \Theta_2 = 45^\circ$, the thread orientation in the frame is

$$\eta = \frac{1}{2} \cos^4 \Theta_1 + \frac{1}{2} \cos^4 \Theta_2 = \frac{1}{4} \quad (2.2)$$

The Poisson ratio can be expressed as

$$\nu_{xy} = \nu_f V_f + \nu_m V_m \quad (2.3)$$

where ν_f is the Poisson ratio of the stainless steel (0.28) and ν_m is the Poisson ratio of the emulsion (0.43) (Irgens, 2008).

In our study, SD75/36 stainless steel screen was utilised with the mesh number of 230 and open area of 46%. The schematic view of the screen cross section is shown in Fig. 2, where d is the diameter of the thread, α is the bending angle, x is the element length of the thread

$$x = \frac{d}{\sin \alpha} \quad (2.4)$$

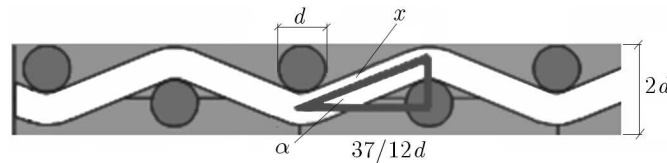


Fig. 2. A sketch of the SD75/36 screen cross section with the main parameters

Using Eq. (2.4), the volume fraction of the stainless steel can be calculated

$$V_f = 2 \frac{d^2 \pi}{4} l \frac{l}{l + d \sin \alpha} \frac{d}{l + d \sin \alpha} = 0.27 \quad (2.5)$$

Substituting Eq (2.5) into Eq. (2.1), the elastic modulus of the screen turned out to be 13 GPa. The sizes of the screen are 298 mm in width, 328 mm in length and the thickness of it was $72 \mu\text{m}$.

These parameters were utilised in the finite element model.

2.2. Measuring the friction force between the screen and the squeegee

The paste we have applied in our experiment was PC 3000 conductive adhesive paste from Heraeus. In the process of screen printing, the friction force between the screen and the squeegee plays an important role. While the squeegee passes the screen due to the friction force the position of the mask shifts. The individual friction force, measuring setup is shown in Fig. 3.

By this measurement, the relationship between the friction force F_f and the printing speed v and squeegee force F_s was estimated. Every thick film paste is viscous and has a non-Newtonian

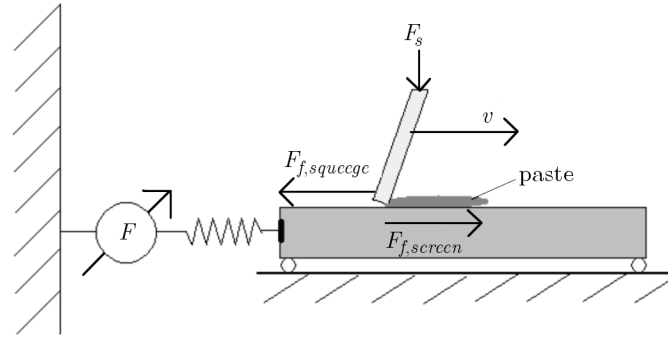


Fig. 3. Measurement setup for determining the friction force between the squeegee

rheology suitable for screen printing. The shear stress τ for this kind of fluids can be described by the Ostwald de Waele relationship

$$\tau = K \left(\frac{dv}{dx} \right)^n \quad (2.6)$$

where K is the flow consistency coefficient [$\text{Pa}\cdot\text{s}^n$], $\partial v/\partial x$ is the shear rate or the velocity gradient perpendicular to the plane of shear [s^{-1}], and n is the flow behaviour index [-] (Scott Blair *et al.*, 1939). Thick film paste is a shear-thinning fluid, thus n is positive, but lower than 1.

In addition, the elongation of the screen – which is greater if the off-contact is greater – results in an image shift as well (Hohl, 1997). The effect of these lateral shifts demonstrated in Fig. 4 has to be taken into account.

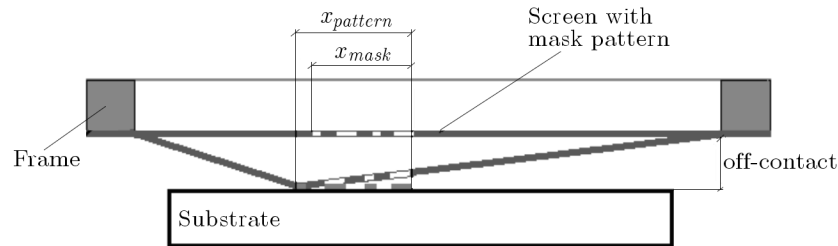


Fig. 4. Deformed paste deposition as a result of screen elongation

The image shift was examined, where the screen tension was in the region of 2-3.3 N/mm, the off-contact was 0.9-1.5 mm, and the applied friction force was based on the measurement.

The reduction of screen tension can affect the quality of the printing in other aspects. The deflection force of the screen is decreasing, so the separation of the substrate and the screen can not start right after the squeegee passes on the screen. This off-contact distance has to be modified in function of screen tension to keep the screen from sticking to the substrate during printing because adhesion causes many separation problems that damage the quality of the printed film.

2.3. Principles of the mechanical model

Equations for mechanical simulations are based on Hook's law for isotropic materials (Bathe, 1996)

$$\boldsymbol{\sigma} = \frac{E}{1+\nu} \left(\boldsymbol{\varepsilon} + \frac{\nu}{1-2\nu} \varepsilon_I \mathbf{I} \right) \quad (2.7)$$

where $\boldsymbol{\sigma}$, $\boldsymbol{\varepsilon}$, ε_I , \mathbf{I} , E , ν parameters are the stress tensor, the strain tensor, the first scalar invariant of it, the identity matrix, Young's modulus and Poisson's ratio, respectively. Due to

the spatial problem of a large thin plate, the general stiffness matrix (used by the finite element software) can be reduced to a simpler form, because the material is symmetric in the x and y direction. The elastic stiffness matrix – according to the circumstances of the given problem – has the following form

$$\mathbf{D} = \frac{E}{(1 + \nu)(1 - 2\nu)} \begin{bmatrix} 1 - \nu & \nu & 0 \\ \nu & 1 - \nu & 0 \\ 0 & 0 & \frac{1 - 2\nu}{2} \end{bmatrix} \quad (2.8)$$

where E is the Young modulus, and ν is the Poisson ratio.

As a consequence of the squeegee load, the screen bends and gets large displacement, so geometric nonlinearity has to be taken into account. Green-Lagrangian strain components E_{ij} can be expressed as

$$E_{ij} = \frac{1}{2} \left(\frac{u_i}{x_j} + \frac{u_j}{x_i} + \frac{u_k}{x_i} \frac{u_k}{x_j} \right) \quad (2.9)$$

where \mathbf{u} is the displacement vector. In the numerical computation, Cauchy stress was calculated.

2.4. Constructing and verifying the Finite Element Model

For the screen model, the shell element was selected because it handles nonlinear geometry in large strain/deflection and in stress stiffening. These two types of geometric nonlinearities are playing a significant role in the modelling of mechanical description of the screen.

SHELL93 element has 6 DOF (degrees of freedom) at each node.

The first step in the modelling of the screen was to determine the initial strain in the screen without an additional load (without the squeegee load), due to the fact it is tighten on the frame. These loads were applied on two perpendicular edges of the screen, while the two others were fixed in the direction of the load acting on the opposite edge. The schematic view of the sizes ($x = 328$ mm, $y = 298$ mm), edge loads (σ_x, σ_y) and constraints only for pretension can be seen in Fig. 5.

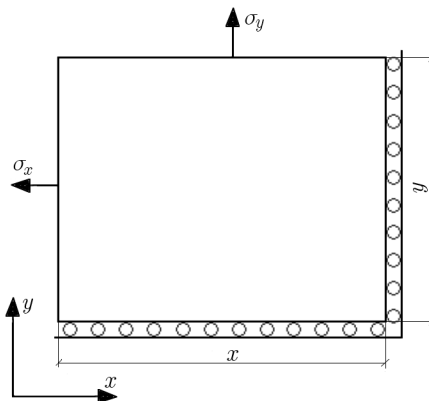


Fig. 5. Layout of the pre-stress condition

In the second model – in which the bending of the screen (resulted by the squeegee load) is calculated in function of the load value and position – the screen tightness is given by a displacement constraint calculated in the model before. As boundary conditions, fixed screen edges (in all directions the displacements and rotations are zero) with the calculated displacement conditions were given. Taking into consideration that the printing process is slow enough, it can be handled stationary in each moment while the screen is in force equilibrium. The width of

the squeegee was 180 mm. Rectangular elements were used and the mesh density was gradually increasing only towards the load area of the squeegee for faster convergence. The aim of this simulation was to examine how the model describes the real process.

In order to compare the FEM calculation to the real situation, a measurement set-up was designed and realised (Fig. 6).

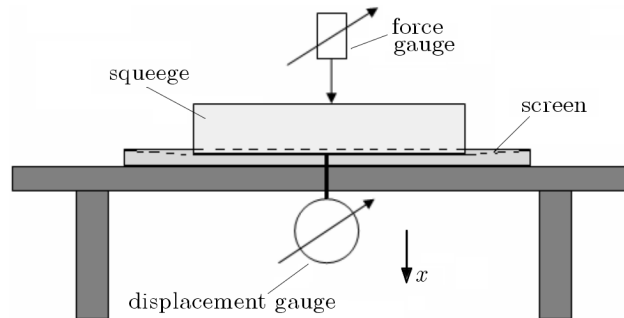


Fig. 6. A sketch of the equipment for measuring deformation of the screen

The screen was loaded at 11 different positions, where the distances from the centre are from 0 mm to 100 mm with 10 mm step size represented in Fig. 7. The load was 40-80 N in 10 N step sizes. These parameters give 55 different measurement points. At one measurement point, 5 measurements were recorded.

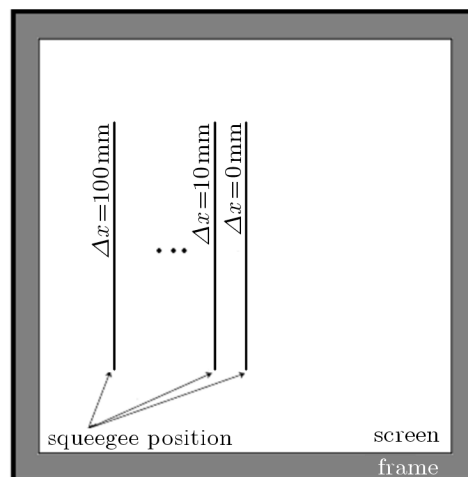


Fig. 7. Squeegee line locations on the screen during the measurement

In the model of screen-printing, the displacement of the screen at the load place in the z direction was maximised according to the industrial standards of distance (about 1 mm) between the screen and the substrate (off-contact) (White *et al.*, 2006). The original construction of the screen printing is shown on Fig. 8.

As boundary conditions, fixed screen edges (motion is zero in all possible directions) were set with the displacement load in the x and y direction, which corresponds to screen tension. In order to simplify the model and to reduce the run time, the contact problem was avoided by using a prescribed displacement load of the screen at the load line. This could be utilized because the screen takes the shape of the squeegee (Fig. 9a). A finer mesh was created in that area where the squeegee acts, and a coarser mesh for the rest of the model (Fig. 9).

The finer-meshed area ensures the accuracy, and the coarser-meshed area provides a faster run time.

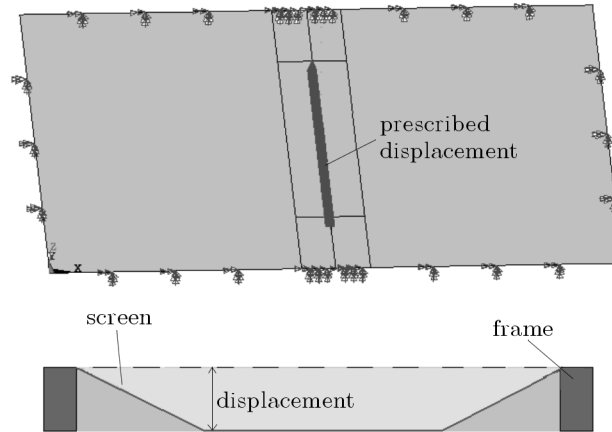


Fig. 8. The original construction of screen printing in the FEM model with constraints

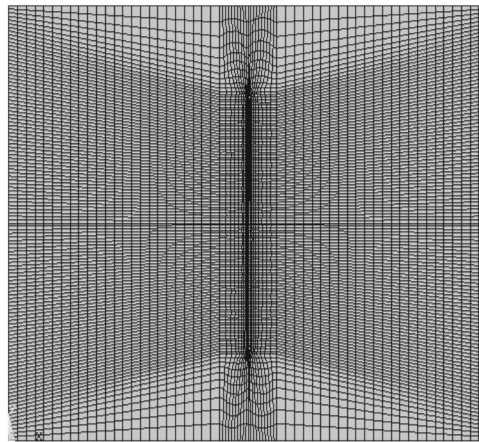


Fig. 9. Meshed screen in FEM; the mesh is densified at the load area of the squeegee

3. Results and discussion

3.1. Modelling of stress distribution in the screen

In the first model of the screen, the initial strain – occurred by the stretching on the frame – was determined. For the initial stress of $\sigma_x = \sigma_y = 2.65 \text{ N/mm}$, displacements in the x and y directions were -0.6209 mm and 0.5641 mm , respectively. In the second model, the screen tightness was given by this displacement constraint calculated in the model before. In this model, the screen was loaded at 11 different positions and 5 different loads according to the measurements. Compared to the simulation results and measurements the screen deformation can be seen on Fig. 10 for 55 different conditions.

In the model of screen printing – where the maximum displacement of the screen in the z direction was 1 mm – the stress was concentrated at the ends of the load area (Fig. 11).

The maximum stress in the screen (105 MPa) appeared around the load edge, while the average stress in the screen was only about 38 MPa . This phenomenon occurred due to the point ending of the squeegee shape, so the corners of the squeegee generate stress concentration in the screen.

The surface quality of the used (5000 cycles) screen was examined by an optical microscope to detect the damage resulted by these high stress peaks (Fig. 12). The investigation shows that the screen area, where the edges of the squeegee passed the filaments, are abraded, however, the middle part is intact.

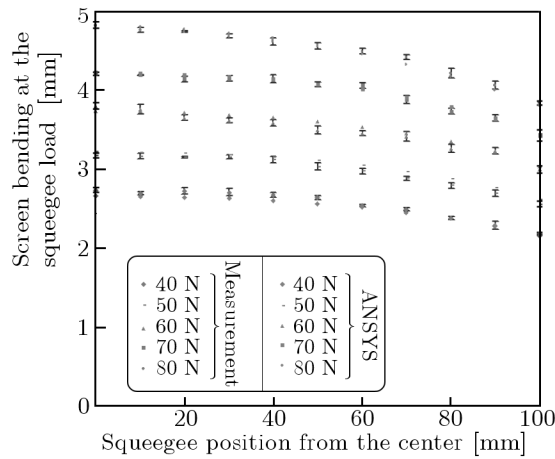


Fig. 10. Measured and simulated bending of the screen at the load line

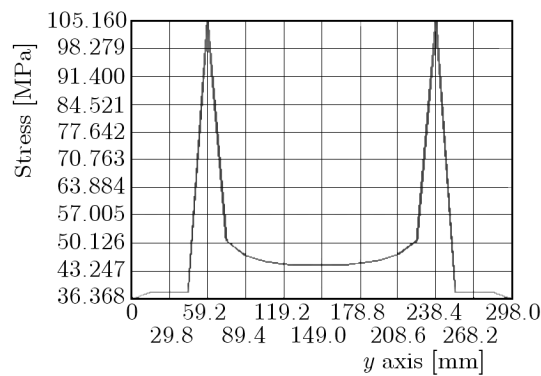


Fig. 11. Mises equivalent stress distribution in the screen along the line to which the load is applied

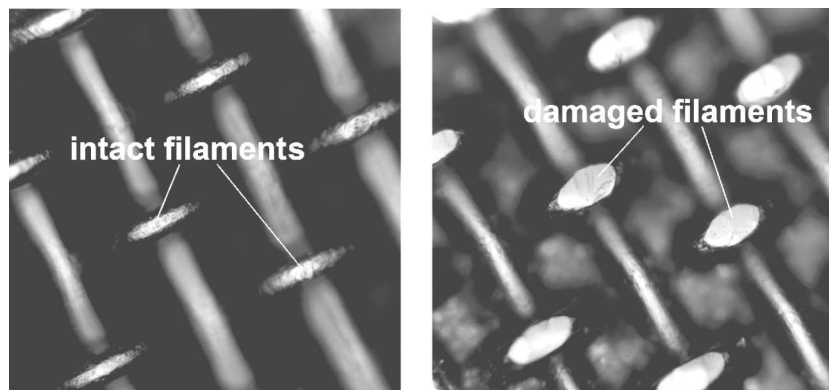


Fig. 12. The middle part of the screen is intact, but where the squeegee edges act, the filaments are abraded

In order to reduce this relative high stress peak in the material, the shape of the squeegee was modified. The two parameters of the round off are R and f , the radius of the circle and the width of the rounded squeegee segment, respectively (Fig. 13).

In the finite element model related to the squeegee round off (further on: fillet), the displacement was prescribed only in the line segment, where the squeegee contacts the screen. This could be utilized here as well because the screen takes the shape of the squeegee to the point P , where the deformed screen profile is tangent to the fillet curve. Here, the condition $\alpha = \beta$ is satisfied (Fig. 14).

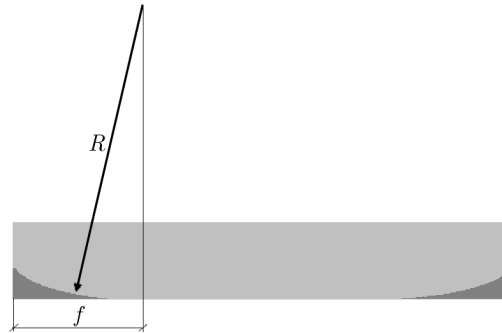


Fig. 13. A scheme of the squeegee round off with the radius of the circle and the width of the rounded squeegee segment

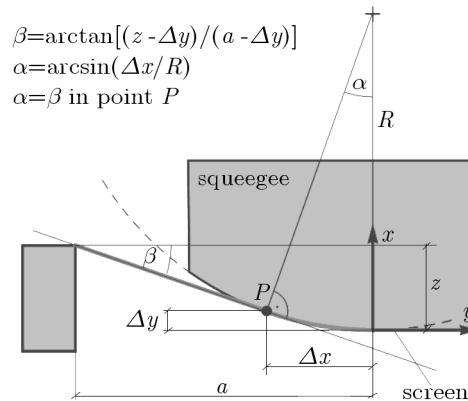


Fig. 14. The prescribed displacement condition of the screen at the line segment where the squeegee contacts the screen

The optimal radius can be obtained from the extrema (in this case, the minimum) of the $\sigma(R)$ stress-radius function (Fig. 15).

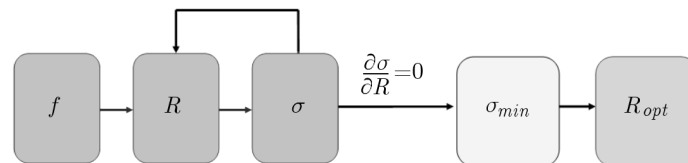


Fig. 15. Process flow of the squeegee – round off optimisation

As a result of rounding squeegee ends for $f = 40$ mm with the optimal R of 1900 mm, the maximum stress in the screen reduced to halves (Fig. 16).

The value of f should be as high as the screen mask allows, because a larger rounded area results in lower stress concentration.

3.2. Effect of the friction force and screen tension on the quality of screen printing

The model was extended with the friction force (see Section 2.2) in order to determine the shift of the pattern of the screen. Table 1 summarises the friction force between the screen and the squeegee in function of the squeegee force and speed.

Evaluating the results from Table 1, it can be determined by regression of the least squares method that n is between 0.2 and 0.4 in Eq. (2.6) for this type of adhesive paste.

Even if the applied friction force was 8.4 N, the off-contact was 1.5 mm and the tension of the screen was reduced to only 2 N/mm, and the resulting shift was less than 2.7 μm .

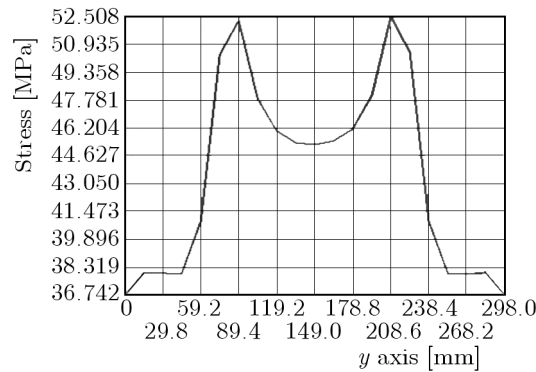


Fig. 16. Mises equivalent stress distribution in the screen along the line of load action

Table 1. The friction force between the screen and the squeegee*

Squeegee pressure [N]	Speed [mm/s]							
	20	40	60	80	100	120	140	160
10	2.2	3.4	4	4.6	4.6	5.2	5.6	5.6
20	2.6	4	4.4	5.2	5.4	5.6	6	6.2
30	3.4	4	4.6	5.2	5.6	5.8	6.8	6.6
40	3.6	4.2	5	5.4	5.8	6	6.8	7
50	3.6	4.6	5	5.4	5.8	6.2	7	7
60	3.8	4.6	5.2	6	5.8	6.4	7.2	7.4
70	4.6	5	5.6	6.2	6.2	6.6	7.4	8
80	4.8	5.6	5.8	6.6	6.6	6.9	8.4	8.4

* at different squeegee forces and speeds

The image deformation arises from the elongation of the screen that is less than $0.5 \mu\text{m}$ in the printing area of the screen in the case of 1.5 mm off-contact. Obviously, it is lower if the off-contact is lower. Accordingly, the deposition shift is negligible under 1.5 mm off-contact, and if the friction force is in this region. However, if there is not enough paste on the screen, the friction force can be multiplied, so the shift can reach $10 \mu\text{m}$.

On the other hand, the quality of printing is maintainable if the reduction of screen tension is compensated. The screen tension is reduced in the screen caused by repetitive printing – which can be handled as a cyclic mechanical load – the elongation of the screen then increases. As the tension is decreasing, the deflection force of the screen is also decreasing, so the screen usually adheres to the substrate and the separation can not start right after the squeegee passes on the screen. The deflection force is maintainable if the off-contact distance is modified.

In our study, the initial screen tension was 3 N/mm and the off-contact was the industrial standard (1 mm), which resulted in the paper printing quality.

In order to avoid adhering, the off-contact has to be increased according to Fig. 17.

As the squeegee force has not been changed, the paste is being printed with the same pressure, and due to the modified off-contact, the elastic force resulting from screen deflection and the paste adhesion has the same force condition as at the initial screen tension and off-contact.

4. Conclusion

A finite element model was created and verified to describe the stress distribution in the screen due to squeegee load. The boundary displacement condition was determined in the first step by a preliminary model. Using these results, a model was constituted to simulate the bending

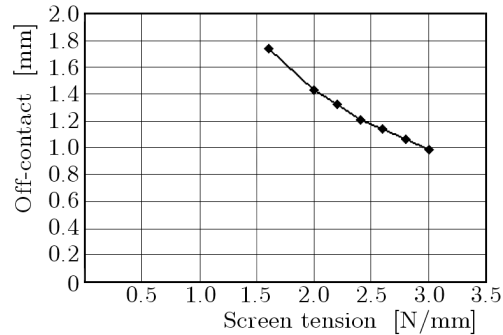


Fig. 17. Off-contact compensation in function of screen tension

of the screen due to different loads acting at different positions. A measurement set-up was designed and realised to verify the model. Comparing the measured and simulated results, it can be clearly concluded that the model gives good approximation of the bending values. In the model of screen printing – where the maximum displacement of the screen in the z direction was 1 mm – the stress was determined. The maxima appeared at the ends of the load area. The geometric parameters of the squeegee were modified to reduce the stress in the screen in order to extend its life cycle. By this, the maximum and the average stress in the screen could be reduced. Furthermore, the decreasing screen tension was compensated by modifying the value of the off-contact, which resulted in a sustainable screen-printing quality. Therefore, the life cycle of the screen could be extended by decreased mechanical stress and increased off-contact.

Acknowledgement

This work has been connected to the scientific program of the "Development of quality-oriented and harmonized R+D+I strategy and functional model at BME" project. This project is supported by the Szechenyi Development Plan (Project ID: TÁMOP-4.2.1/B-09/1/KMR-2010-0002). This paper has been supported by Janos BOLYAI fellowship of HAS (Hungarian Academy of Science). The authors would like to thank Hatvan – Robert Bosch Elektronika Ltd. for funding the project.

References

1. ALBAREDA-SIRVENT M., MERKOÇI A., ALEGRET S., 2000, Configurations used in the design of screen-printed enzymatic biosensors. A review, *Sensors and Actuators B: Chemical*, **69**, 1/2, 153-163
2. BACHER R.J., 1986, High resolution thick film printing, *Proceedings of the International Symposium on Microelectronics*, 576-581
3. BATHE K.-J., 1996, *Finite Element Procedures*, Prentice Hall
4. BENSON M.A., 1969, Thick-film screen printing, *Solid State Technology*, 53-58
5. COX H.L., 1952, The elasticity and strength of paper and other fibrous materials, *British Journal of Applied Physics*, **3**, 72-79
6. HOHL D., 1997, Controlling off-contact, *Specialty Graphic Imaging Association Journal*, **4**, 5-11
7. IRGENS F., 2008, *Continuum Mechanics*, Springer
8. JEONG J., KIM M., 1985, Slow viscous flow due to sliding of a semi-infinite plate over a plane, *Journal of Physics Society*, **54**, 1789-1799
9. KOBIS D.R., VOIGT D.R., 1970, Parametric dependencies in thick film screening, *Proc. ISHM*, **18**, 1-10

10. KREBS F.C., 2007, Large area plastic solar cell modules, *Materials Science and Engineering: B*, **138**, 2, 106-111
11. KRENCHER H., 1964, *Fibre Reinforcement*, Akademisk Forlag, Copenhagen, Denmark
12. MILLER L.F., 1969, Paste transfer in the screening process, *Solid State Technology*, 46-52
13. RIEDLER J., 1983, Viscous flow in corner regions with a moving wall and leakage of fluid, *Acta Mechanica*, **48**, 95-102
14. RIEMER D.E., 1988a, Analytical model of the screen printing process: part 1, *Solid State Technology*, **8**, 107-111
15. RIEMER D.E., 1988b, Analytical model of the screen printing process: part 2, *Solid State Technology*, **9**, 85-90
16. RIEMER D.E., 1989, The theoretical fundamentals of the screen printing process, *Hybrid Circuits*, **18**, 8-17
17. SCOTT BLAIR G.W., HENING J.C., WAGSTAFF A., 1939, The flow of cream through narrow glass tubes, *Journal of Physical Chemistry*, **43**, 7, 853-864
18. TAYLOR G.I., 1962, On scraping viscous fluid from a plane surface, *Miszallangen Angewandten Mechanik*, 313-315
19. VIRICELLE J.P., 2006, Compatibility of screen-printing technology with microhotplate for gas sensor and solid oxide micro fuel cell development, *Sensors and Actuators B: Chemical*, **118**, 1/2, 263-268
20. WHITE G.S., BREWARD C.J.W., HOWELL P.D., 2006, A model for the screen-printing of Newtonian fluids, *Journal of Engineering Mathematics*, **54**, 49-70

Modelowanie mechaniczne i optymalizacja żywotności siatki w technologii druku sitowego obwodów mikroelektronicznych

Streszczenie

Upowszechnioną na skalę masową metodę nakładania warstw klejów i materiałów adhezyjnych w technologii grubowarstwowej oraz niskotemperaturowo współspiekanych obwodów drukowanych na płytkach ceramicznych jest druk sitowy. Za pomocą tej technologii, substancja klejąca nakładana jest na powierzchnię substratu gumowym raklem, przeciskającym klej przez siatkę wykonaną ze stali nierdzewnej pokrytej emulsją fotolitograficzną. W pracy omówiono bezstykową wersję sitodruku, ponieważ jest ona obecnie standardową techniką stosowaną w przemyśle mikroelektronicznym. W prezentowanej pracy wygenerowano w systemie ANSYS model elementów skończonych badanej siatki do określenia jej odkształceń i oceny możliwości ograniczenia poziomu naprężeń pod kątem zwiększenia żywotności. Opracowano i wytworzono indywidualną aparaturę pomiarową do weryfikacji stanu odkształcenia obliczonego modelem MES. W wyniku badań stwierdzono, że zaproponowana modyfikacja geometrii rakla pozwala obniżyć maksymalne i średnie naprężenia w siatce. Obserwowanym zjawiskiem jest także stopniowa utrata napięcia siatki w trakcie normalnej eksploatacji, co prowadzi do pogorszenia jakości sitodruku. Zmodyfikowany kształt rakla kompensuje ten efekt i wydłuża żywotność siatki poprzez obniżenie wartości naprężeń i zoptymalizowanie parametrów geometrycznych druku bezstykowego.

Manuscript received December 7, 2011; accepted for print February 2, 2012